Fe^{III}-Hydroperoxo and Peroxo Complexes with Aminopyridyl Ligands and the Resonance Raman Spectroscopic Identification of the Fe−O and O−O Stretching Modes

A. Jalila Simaan,[a] Susanne Döpner,[b] Frédéric Banse,[a] Sophie Bourcier,[c] Guy Bouchoux,[c] Alain Boussac,[d] Peter Hildebrandt,*[b] and Jean-Jacques Girerd*[a]

Keywords: Iron / Peroxides / Nonheme iron models / Raman spectroscopy

Nonheme Fe^{III}-hydroperoxo and Fe^{III}-peroxo complexes with aminopyridyl-type ligands have been prepared and characterized by UV/Vis, EPR, mass and Resonance Raman (RR) spectroscopy. The $Fe^{III}(OOH)$ species are low-spin and exhibit a deep purple color due to the ligand-to-metal charge transfer (LMCT) band centered at ca. 550 nm. The RR spectra of the $Fe^{III}(OOH)$ complexes display two bands at ca. 620 and 800 cm^{-1} that are assigned to the respective Fe–O and O–O stretching modes on the basis of the characteristic H/D and $^{16}O/^{18}O$ frequency shifts. Upon deprotonation, $Fe^{III}(O_2)$ species are obtained which possess a high-spin configuration of nearly axial symmetry and a LMCT transition in the near infrared (ca. 750 nm). The frequencies of the Fe–O and O–O stretching modes at ca. 465 and 820 cm^{-1}, as well as their respective $^{16}O/^{18}O$ shifts of –16 and –45 cm^{-1}, indicate an η^2 coordination geometry for the $Fe^{III}(O_2)$ complex.

Introduction

The currently proposed mechanism for catalytic oxygenation by cytochrome P450 involves an Fe^{III}-peroxo intermediate that leads, upon protonation, to a ferryl species which is able to insert an oxygen atom into a C−H bond.[1] Whereas the Fe^{III}-peroxo species has been observed during the enzymatic reaction cycle, identification of the ferryl species has not yet been possible due to its high reactivity.[2] For nonheme systems such as bleomycin,[3] a ferryl species may also be implied, although in this case experimental proof has not yet been presented either. Specifically, the intermediate state denoted as "activated bleomycin" has been recently shown to be $(BLM)Fe^{III}(OOH)$.[4] In order to understand the reactivity of such nonheme hydroperoxoiron species, several chemical models have been prepared and studied.[5−14]

A well-known example of a nonheme Fe^{III}-peroxo complex is $[(EDTA)Fe^{III}(O_2)]^{3-}$.[15,16] Spectroscopic studies demonstrated a side-on coordination of the peroxo group in this complex. We recently reported the formation of a new type of nonheme Fe^{III}-peroxo complex using the ligand [*N*-methyl-*N*,*N*′,*N*′-tris(2-pyridylmethyl)ethane-1,2-diamine] (trispicMeen).[17] This Fe^{III}-peroxo species was obtained by deprotonation of the Fe^{III}-hydroperoxo complex.[8,11] Analogous species were obtained by Jensen et al.[14] RR spectroscopic studies by Ho et al.[18] indicated an η^2-coordination of the peroxo group in $[(N4py)Fe^{III}(O_2)]^+$.

The present study is dedicated to the RR spectroscopic characterization of the hydroperoxo and peroxo species of Fe^{III} complexes formed with trispicMeen as well as of the corresponding Fe^{III} complexes involving the ligands [*N*,*N*′,*N*′-tris(2-pyridylmethyl)ethane-1,2-diamine] (trispicen) and [*N*,*N*,*N*′,*N*′-tetrakis(2-pyridylmethyl)ethane-1,2-diamine] (TPEN) (Scheme 1).

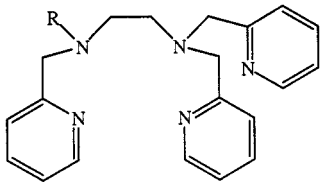

R = H trispicen
R = Me trispicMeen
R = CH_2Py TPEN

Scheme 1. Ligands used in this study

Results and Discussion

The starting materials for preparing the hydroperoxo and peroxo species are Fe^{II} complexes. For the complex with the trispicMeen ligand, [(trispicMeen)FeCl]Cl was used as starting material.[17] The structure of the related species

[a] Laboratoire de Chimie Inorganique, UMR CNRS 8613, Université Paris-Sud, 91405 Orsay, France
[b] Max-Planck-Institut für Strahlenchemie, D-45470 Mülheim/Ruhr, Germany
[c] Laboratoire des Mécanismes Réactionnels, UMR CNRS 7651, Ecole Polytechnique, 91128 Palaiseau, France
[d] Section de Bioénergétique, URA CNRS 2096, CEA Saclay, 91191 Gif-sur-Yvette, France

  1434−1948/00/0707−1627 $ 17.50+.50/0

[(trispicMeen)FeCl]BPh_4 has been recently determined.[11] For the complexes with the ligand trispicen, [(trispicen)-FeCl]PF_6 served as starting material. In the case of the TPEN ligand, the parent complex was prepared in THF and isolated as a yellow powder, the analysis of which corresponds to [(TPEN)Fe]$Cl_2 \cdot 0.5H_2O$. The yellow color and the magnetic susceptibility, measured as a function of temperature,[19] demonstrate a ferrous high-spin state which may be indicative of the coordination of chloride to Fe^{II}, i.e. [(TPEN)FeCl]$Cl \cdot 0.5H_2O$. In MeOH, an orange color was obtained and the UV/Vis spectrum was identical to that of [(TPEN)Fe]$(ClO_4)_2$ in the same solvent, suggesting dissociation of the chloride ligand in solution to give the $[(TPEN)Fe]^{2+}$ complex. The structure of [(TPEN)-Fe]$(ClO_4)_2$ has been previously published.[20]

UV/Visible Absorption Spectroscopy

The species containing the $Fe^{III}OOH$ unit absorb around 550 nm (Table 1) as already reported for [(trispicMeen)-$Fe(OOH)]^{2+}$.[8] Upon deprotonation, [(trispicMeen)Fe-$(O_2)]^+$ is formed which gives an absorption band at much lower energy (740 nm, Table 1).[14,17] The same observations were made for the corresponding transformation of $[(TPEN)Fe(OOH)]^{2+}$ to $[(TPEN)Fe(O_2)]^+$ (Figure 1). These bands are attributed to LMCT transitions from the HO_2^- or O_2^{2-} groups to Fe^{III}.

Table 1. Characteristics of the LMCT band in MeOH for the different complexes

Complex	λ_{max} (ε/м$^{-1}$.cm^{-1})	ref.
Hydroperoxo		
$[(trispicMeen)Fe(OOH)]^{2+}$	537 nm (1000)	[8][11]
$[(trispicen)Fe(OOH)]^{2+}$	531 nm (950)	this work
$[(TPEN)Fe(OOH)]^{2+}$	541 nm (900)	this work
Peroxo		
$[(trispicMeen)Fe(O_2)]^+$	740 nm (500)	[17]
$[(TPEN)Fe(O_2)]^+$	755 nm (450)	this work

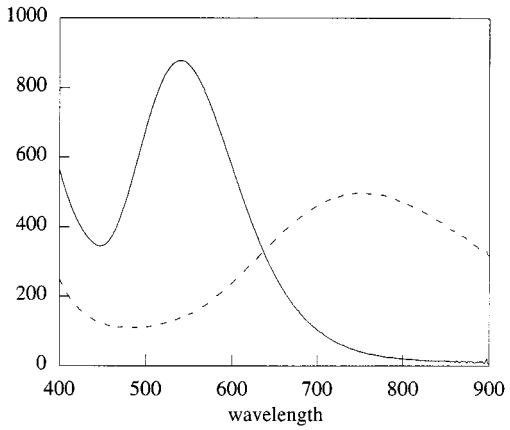

Figure 1. UV/Vis spectra of $[(TPEN)Fe^{III}(OOH)]^{2+}$ (1 мм in MeOH, 100 equiv. of H_2O_2) before ( ) and after addition of three equiv. of NEt_3 (− − −) measured at ambient temperature; the bands at 541 nm and 755 nm are attributed to the LMCT transitions of $[(TPEN)Fe^{III}(OOH)]^{2+}$ and $[(TPEN)Fe^{III}(O_2)]^+$, respectively

The formation of the purple complex [(trispicen)-$Fe(OOH)]^{2+}$ in MeOH was monitored by UV/Vis spectroscopy. Upon addition of base, the purple color disappeared although we failed to trap the putative $[(trispicen)Fe(O_2)]^+$ species.

EPR Spectroscopy

The $Fe^{III}OOH$ species display EPR spectra that are typical for ferric low-spin (LS) states. At 100 K, the g values of $[(trispicen)Fe(OOH)]^{2+}$ and $[(trispicMeen)Fe(OOH)]^{2+}$ were observed at 2.19, 2.14, 1.96 and at 2.19, 2.12, 1.95, respectively.[8,11] For $[(TPEN)Fe(OOH)]^{2+}$, we have found resonances at 2.22, 2.15, 1.967 (Figure 2).

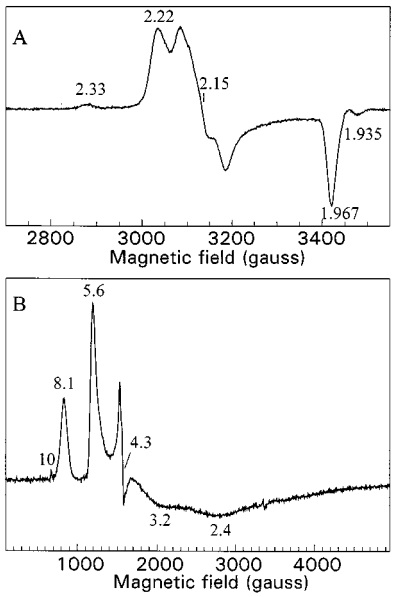

Figure 2. A: EPR spectrum of $[(TPEN)Fe^{III}(OOH)]^{2+}$ in MeOH measured at 15 K; B: EPR spectrum of $[(TPEN)Fe^{III}(OOH)]^{2+}$ in MeOH at 4 K in the presence of three equivalents of NEt_3; the signal at $g = 4.3$ corresponds to a degradation product

It is possible to describe the g values for a LS Fe^{III} by using the model of Griffith[21] as presented by Taylor,[22] which takes into account the spin-orbit coupling and distortion from octahedral geometry. These effects lift the six-fold degeneracy of the $^2T_{2g}$ ground state and three well-separated Kramers doublets are obtained. This corresponds to a lifting of the orbital degeneracy, as indicated in Scheme 2, where the rhombic and axial distortion energies are denoted by V and Δ, respectively.

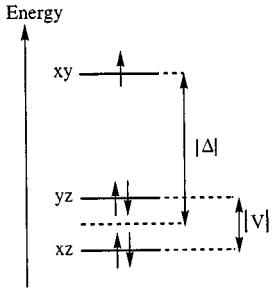

Scheme 2. Splitting of the T_{2g} orbitals due to distorsions

Table 2. EPR g_{max}, g_{inter}, g_{min} values for $Fe^{III}OOH$ $s = 1/2$ units; parameters of the Griffith−Taylor model of the g tensor: *a, b, c* are the coefficients of the wavefunctions; $\Sigma = a^2 + b^2 + c^2$; V is the rhombic distorsion energy; Δ is the axial distorsion energy; both are in units of λ, the spin-orbit coupling constant

complex	$-g_{min}$, g_z	g_{max}, g_y	$-g_{inter}$, g_x	*a*	*b*	*c*	Σ	V/λ	Δ/λ
(BLM)Fe(OOH)	−1.94	2.26	−2.17	0.072	0.052	0.993	0.993	3.04	−8.74
$[(trispicMeen)Fe(OOH)]^{2+}$	−1.95	2.19	−2.12	0.055	0.039	0.992	0.988	4.05	−11.31
$[(trispicen)Fe(OOH)]^{2+}$	−1.96	2.19	−2.14	0.053	0.041	0.994	0.993	2.86	−11.19
$[(TPEN)Fe(OOH)]^{2+}$	−1.967	2.22	−2.15	0.056	0.040	0.999	1.002	3.98	−11.29

At 100 K, only the lowest doublet is populated. The two wave functions of the ground Kramers doublet are written as:

$$|+> = a\,|\xi\alpha> - i\,b\,|\eta\alpha> - c\,|\zeta\beta> \quad (1)$$

$$|-> = -a\,|\xi\beta> - i\,b\,|\eta\beta> - c\,|\zeta\alpha> \quad (2)$$

where $|\xi\alpha>$, $|\eta\alpha>$, $|\zeta\beta>$ refer to the states with the unpaired electron in the d_{yz}, d_{xz}, and d_{xy} orbital, respectively. The associated g values are given by:[22]

$$g_z = 2[(a + b)^2 - c^2] \quad (3)$$

$$g_y = 2[(a + c)^2 - b^2] \quad (4)$$

$$g_x = 2[a^2 - (b + c)^2] \quad (5)$$

These equations were used to evaluate the constants a, b, and c assuming that $g_x\,g_y\,g_z$ is positive. This assumption, originally suggested by Veselov et al.,[23] appears to be justified in view of the chemical meaning of the results. The a, b and c values were calculated from the experimental g values. As described by Taylor[22] we selected the axes such that $|V| < (2/3)\,|\Delta|$. The results are presented in Table 2.

For (BLM)$Fe^{III}OOH$, values of $g_z = -1.94$, $g_y = 2.26$, and $g_x = -2.17$ were found corresponding to $a = 0.072$, $b = 0.052$, and $c = 0.993$ with $V/\lambda = 3.04$ and $\Delta/\lambda = -8.74$. These values imply that the hole (and hence the unpaired electron) is in an orbital which has predominantly d_{xy} character, and that this orbital is strongly destabilized. The d_{xz} and d_{yz} orbitals would be lower in energy, with the d_{xz} being the lowest. Based on an ENDOR study of activated bleomycin, Veselov et al.[23] suggested, by comparison with LS hemes, that the axis of g_{max} (y from the calculation above) is perpendicular to the conjugated pyrimidine plane and parallel to the Fe-peroxo axis. This conclusion is not in contradiction with the above discussion and leads to the following proposal for the orientation of the g tensor (Scheme 3).

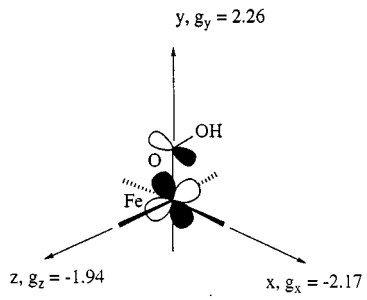

Scheme 3. Nature of the singly occupied T_{2g} orbital and orientation of the g tensor

The values for $[(trispicMeen)Fe(OOH)]^{2+}$ are similar to those of (BLM)$Fe^{III}OOH$ with $g_z = -1.95$, $g_y = 2.19$, $g_x = -2.12$, $a = 0.055$, $b = 0.039$, $c = 0.992$, $V/\lambda = 4.05$, $\Delta/\lambda = -11.31$. Thus, in analogy to bleomycin, it is concluded that in this model complex the unpaired electron is also in a d_{xy} type orbital. Note that the axial perturbation is stronger in the model complexes than in the activated bleomycin. This different behavior may be due to the stronger π-acceptor capability of the ligand in the model complexes so that the interaction between the d_{xy} type orbital and the π* orbital of OOH becomes stronger.

The $Fe^{III}-O_2$ species are high spin ($S = 5/2$) with resonances at $g = 7.5$ and 5.9 as determined for $[(trispicMeen)Fe(O_2)]^+$.[17] The $g = 7.5$ signal can be interpreted as arising from the upper Kramers doublet with $E/D = 0.08$ for $D < 0$, whereas the $g = 5.9$ signal may arise from the intermediate Kramers doublet.[17] The complex $[(TPEN)Fe(O_2)]^+$ displays resonances at $g = 10$, 8.1, 5.6, 3.2, 2.4 (Figure 2). These signals are due to the different Kramers doublets with $E/D = 0.10$ for $D < 0$. The $g = 10$ signal is tentatively assigned to the ground doublet whereas the signals at $g = 5.6$ and $g = 2.4$ may originate from the intermediate doublet. The $g = 8.1$ and $g = 3.2$ may then be attributed to the upper doublet. These findings suggest that $[(trispicMeen)Fe(O_2)]^+$ and $[(TPEN)Fe(O_2)]^+$ have similar structures.

Mass Spectrometry

$[(TrispicMeen)Fe(OOH)]^{2+}$ and $[(trispicMeen)Fe(O_2)]^+$ have been detected by Electrospray Ioniation Mass Spectrometry.[11,17] After addition of three equivalents of Et_3N to a purple 10^{-3} M solution of $[(TPEN)Fe(OOH)]^{2+}$ in methanol, the ESI-MS spectrum (Figure 3) exhibits a major peak at $m/z = 512.3$ which can be attributed to $[(TPEN)Fe^{III}(O_2)]^+$. Among the other peaks detected, those at $m/z = 425.3$ and 542.3 are assigned to ($TPENH^+$) and ($[(TPEN)Fe^{III}(OMe)_2]^+$), respectively. The peak at $m/z = 512.3$ disappears after 10 min, which parallels the disappearance of the blue color of the solution.

Resonance Raman Spectroscopy

Excitation in resonance with the LMCT transitions should provide a preferential enhancement of the vibrational modes originating from the iron-(hydro)peroxo entities, which is indeed confirmed by the present experiments. The RR spectra of the hydroperoxo complexes were recorded with excitation at 568 nm. The spectral regions be-

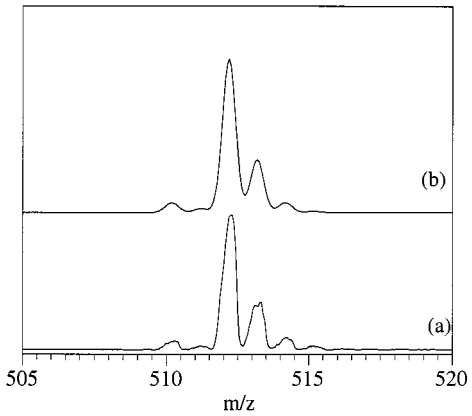

Figure 3. EI-MS features of $[(TPEN)Fe^{III}(O_2)]^+$ at m/z = 512.3: a) experimental spectrum; b) calculated spectrum

tween 570 and 640 cm^{-1} and 710 and 880 cm^{-1}, which are expected to include the iron−oxygen and oxygen−oxygen stretching modes, respectively, are shown in Figure 4 for the $[(trispicMeen)Fe(OOH)]^{2+}$ complex. The former region displays two bands at 617 cm^{-1} and 632 cm^{-1} that are possible candidates for the Fe−O stretching. The 617 and 632 cm^{-1} bands are not detected in the spectrum of the parent state, i.e. prior to the addition of H_2O_2, implying that both bands originate from the $[(trispicMeen)Fe(OOH)]^{2+}$ complex or derivatives thereof. The dominant band at 617 cm^{-1} shifts to lower wavenumbers 613 and 600 cm^{-1} upon H/D exchange and ^{18}O-labeling, respectively (Table 3). These shifts are consistent with the calculated values obtained from a simple two-body oscillator model for the Fe−OOH moiety of the presumed hydroperoxo complex.

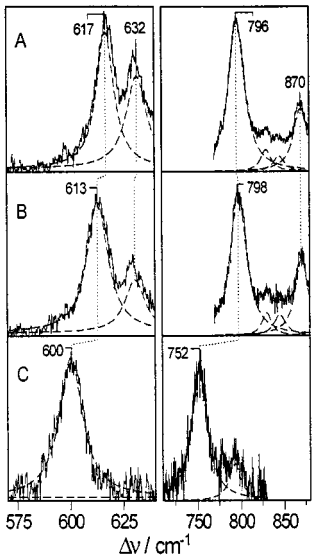

Figure 4. RR spectra of $[(trispicMeen)Fe(OOH)]^{2+}$ obtained with 568 nm excitation. (A) natural abundance, complex prepared with H_2O_2; (B) deuterated, complex prepared with D_2O_2; (C) ^{18}O-labeled, complex prepared with $H_2{}^{18}O_2$; the regions of the iron−oxygen and oxygen−oxygen stretching modes are displayed in the left and right panels, respectively; the dotted lines represent the fitted Lorentzian bandshapes.

Therefore, the band at 617 cm^{-1} is assigned to the Fe−O stretching mode of the $[(trispicMeen)Fe(OOH)]^{2+}$ complex. The second band in this region at 632 cm^{-1} remains essentially unchanged upon deuteration. The intensity of this band relative to the 617 cm^{-1} band reveals some variations in the different samples and, moreover, increases with time along with the decomposition of $[(trispicMeen)Fe(OOH)]^{2+}$. Samples which have been measured four hours after complex preparation show a broad band centered at ca. 630 cm^{-1} whereas no band can be detected at 617 cm^{-1}. We therefore attribute the band at 632 cm^{-1} to a degradation product of $[(trispicMeen)Fe(OOH)]^{2+}$. Note that this band is hardly detectable in the ^{18}O-labeled complex, which may be due to a relatively small contribution of this degradation product in the sample. The Fe−O frequency at 617 cm^{-1} is in agreement with the value found by Que and co-workers for $[(N4py)Fe(OOH)]^{2+}$ and $[(TPA)Fe(OOH)]^{2+}$.[12,13]

The O−O stretching mode is expected between ca. 770 and 850 cm^{-1}.[12,13] This part of the spectrum also includes a band at 870 cm^{-1} originating from the O−O stretching mode of H_2O_2 (Figure 4). In the deuterated solvent, this band reveals a small shift of 1 cm^{-1} as previously noted.[15] The strongest band in this region, at 796 cm^{-1}, is unambiguously assigned to the O−O stretching mode of $[(trispicMeen)Fe(OOH)]^{2+}$ since it shifts to lower wavenumber (752 cm^{-1}) in the ^{18}O-labeled sample (Table 3), which confirms the predictions for a hydroperoxo complex. Upon H/D exchange this mode reveals a similar shift to that for H_2O_2.[15]

The complex $[(TPEN)Fe(OOH)]^{2+}$ shows essentially the same RR spectra as $[(trispicMeen)Fe(OOH)]^{2+}$ (Figure 5) with nearly identical frequencies for the Fe−O and O−O stretching modes (Table 3). These similarities with $[(trispicMeen)Fe(OOH)]^{2+}$ indicate that the additional pyridyl arm of the TPEN ligand is not involved in the coordination to iron. In contrast, in the RR spectrum of $[(trispicen)Fe(OOH)]^{2+}$ both the Fe−O and the O−O modes are observed at higher frequencies than in $[(trispicMeen)Fe(OOH)]^{2+}$ and $[(TPEN)Fe(OOH)]^{2+}$ (Table 3). Furthermore, the isotopic shifts are also larger. These differences could be related to a different geometry of the FeOOH unit in $[(trispicen)Fe(OOH)]^{2+}$ as a consequence of the reduced steric hindrance upon replacement of the tertiary amino group by a secondary amino group (i.e. R = H vs. R = CH_2py in Scheme 4).

For the investigation of the blue peroxo complexes, excitation at 647 nm, albeit not in rigorous resonance with the LMCT transition, provides a preferential enhancement of the modes associated with the iron peroxo group. In the O−O stretching region, the RR spectrum of $[(trispicMeen)Fe(O_2)]^+$ displays a new band at ca. 819 cm^{-1} which shifts down to 776 cm^{-1} in the ^{18}O-labeled complex but remains unchanged upon H/D exchange so that it is unambiguously assigned to the O−O stretching mode (Figure 6). A careful inspection reveals an asymmetric shape of the 819 cm^{-1} band both in nondeuterated and deuterated solvents but not of the 776 cm^{-1} band of the ^{18}O-labeled species. A band-fitting analysis of the 819 cm^{-1} peak affords a strong band at 819 and a weaker one at 827 cm^{-1}

Table 3. Frequencies of the iron−oxygen and oxygen−oxygen modes of the various iron hydroperoxo and iron peroxo complexes; the accuracies of the frequencies (given in cm^{-1}) are ca. 0.3 cm^{-1} for the hydroperoxo species and ca. 1.0 cm^{-1} for the individual band components of the composite peaks in the peroxo complexes; the abbreviations H/D and $^{16}O/^{18}O$ denote the H/D and $^{16}O/^{18}O$ isotopic shifts

Complex	ν_{Fe-O}	ΔH/D	$\Delta^{16}O/^{18}O$	ν_{O-O}	ΔH/D	$\Delta^{16}O/^{18}O$
Hydroperoxo						
$[(trispicMeen)Fe(OOH)]^{2+}$	617.2	−4.1	−17.0	796.4	+1.2	−44.7
$[(TPEN)Fe(OOH)]^{2+}$	617.2	−3.7	n.d.[a]	795.9	+2.0	n.d.[a]
$[(trispicen)Fe(OOH)]^{2+}$	624.8	−7.1	−22.6	800.7	+0.2	−50.5
Peroxo						
$[(trispicMeen)Fe(O_2)]^{+}$	470	0.0	−16	819	−	−
	−	−	−	−	0.0	−45[b]
	−	−	−	827	−	−
$[(TPEN)Fe(O_2)]^{+}$	470	n.d.[a]	n.d.[a]	817	−	−
	−	−	−	−	n.d.[a]	n.d.[a]
	−	−	−	824	−	−

[a] n.d.: not determined. − [b] The $^{16}O/^{18}O$ shifts refer to shifts of the peak maxima.

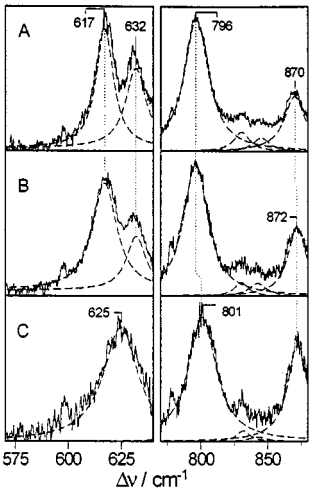

Figure 5. RR spectra of $[(trispicMeen)Fe(OOH)]^{2+}$, $[(TPEN)Fe(OOH)]^{2+}$ and $[(trispicen)Fe(OOH)]^{2+}$ obtained with excitation at 568 nm; the regions of the iron-oxygen and oxygen-oxygen stretching modes are displayed in the left and right panels, respectively; the dotted lines represent the fitted Lorentzian bandshapes

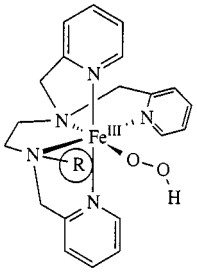

Scheme 4. Proposed structure for the FeOOH complex indicating the possible steric hindrance between the alkyl substituent and the hydroperoxo group

(Table 3). These band components are also found in the $[(TPEN)Fe(O_2)]^{+}$ complex, albeit with slightly different frequencies and relative intensities (Figure 7).

A comparable heterogeneity is observed for the iron−oxygen stretching of $[(trispicMeen)Fe(O_2)]^{+}$ and $[(TPEN)Fe(O_2)]^{+}$ which is attributable to the composite bands centered at 470 cm^{-1} (Figure 6). These bands are not affected by H/D exchange but shift to lower wavenumber by ca. 16 cm^{-1} in the ^{18}O-labeled complex. The relatively

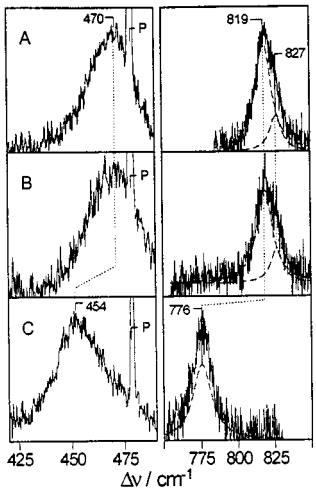

Figure 6. RR spectra of $[(trispicMeen)Fe(O_2)]^{+}$ obtained with excitation at 647 nm: (A) natural abundance, complex prepared with H_2O_2; (B) deuterated, complex prepared with D_2O_2; (C) ^{18}O-labeled, complex prepared with $H_2{}^{18}O_2$; the regions of the iron-oxygen and oxygen-oxygen stretching modes are displayed in the left and right panels, respectively; the dotted lines represent the fitted Lorentzian bandshapes; the sharp peak labeled P originates from a plasma line of the laser

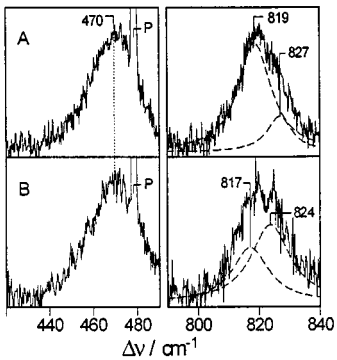

Figure 7. RR spectra of $[(trispicMeen)Fe(O_2)]^{+}$ and $[(TPEN)Fe(O_2)]^{+}$ obtained with excitation at 647 nm; the regions of the iron−oxygen and oxygen−oxygen stretching modes are displayed in the left and right panels, respectively; the dotted lines represent the fitted Lorentzian bandshapes; the sharp peak labelled P originates from a plasma line of the laser

low frequencies of the Fe−O stretches are related to the spin configuration in the peroxo complexes. Whereas the LS configuration in the hydroperoxo complexes allows for the formation of a relatively strong Fe−O bond corresponding to a high Fe−O stretching frequency, the HS configuration of the peroxo complexes leads to a weakening of the Fe−O bond which is reflected by the substantially lower Fe−O stretching frequency.[13]

Both the Fe−O and O−O stretching frequencies and their $^{18}O/^{16}O$ shifts indicate a side-on structure of the iron-peroxo moiety, in agreement with previous findings for Fe^{III} peroxo complexes ligated by EDTA and N4py.[15,16,18] The coexistence of two closely spaced O−O stretching modes, as well as the asymmetric profile of the Fe−O stretching peak, may indicate two conformers which subtly differ in structural details.

Conclusion

All Fe^{III} compounds studied in this work form LS hydroperoxo complexes. Whereas the trispicMeen and TPEN derivatives reveal very similar spectroscopic properties, $[(trispicen)Fe(OOH)]^{2+}$ exhibits somewhat higher Fe−O and O−O stretching frequencies, indicating slightly different molecular structures. This compound evidently also displays a different reactivity since no peroxo complex could be detected at room temperature. It may be that the lifetime of this species is too short due to the sensitivity to oxidation of the secondary amine NH group of the trispicen ligand. In the peroxo complexes of the other compounds, the Fe^{III} adopts an HS configuration. However, the anisotropy of this $S = 5/2$ state depends on the auxiliary ligand. Whereas complexes with N4py and EDTA ligands lead to a rhombic state, a more axial state is found for the Fe^{III}-peroxo complexes formed with trispicMeen and TPEN ligands. Regardless of these differences, the present RR spectroscopic data indicate an η^2-coordination of the peroxo groups in the trispicMeen and TPEN complexes as well, implying that side-on coordination represents a structural motif that is largely independent of the type of auxiliary ligand.

Experimental Section

General: All manipulations were carried out using standard Schlenk techniques. Starting materials were purchased from Acros. Solvents were purchased from Merck and used without further purification. $^{18}O_2H_2$ was provided as a 2% aqueous solution from Leman. − UV/Vis: Varian Cary 5E equipped with a temperature controller. − MS: Quattro II (Micromass, Manchester, UK) triple quadrupole electrospray mass spectrometer. Typical optimized values for the source parameters were: capillary: 2.5 kV, counter electrode: 0.4 kV, cone voltage: 15 to 30 V, source temperature: 80 °C, RF lens: 0.7 V, skimmer lens offset: 5 V. − EPR spectra were recorded on a Bruker ESP 300 E spectrometer. For low-temperature studies, an Oxford Instruments continuous-flow helium cryostat and a temperature control system were used. Magnetic susceptibility measurements in the 10−300 K temperature range were carried out with a MPMS5 SQUID susceptometer (Quantum Design Inc.). The calibration was made at 298 K using a palladium reference sample furnished by Quantum Design Inc.

RR Measurements: RR experiments were carried out at ambient temperature using an U1000 spectrograph (ISA) equipped with 1200 lines/mm gratings and a liquid-nitrogen cooled CCD camera. The spectral bandwidth was 2.8 cm^{-1} and the increment per data point was ca. 0.2 cm^{-1}. The wavenumber stability of the monochromator was 0.1 cm^{-1}. The 568- and 647-nm lines of a Kr^+ laser, with a power 25 and 50 mW, respectively, at the sample were used for excitation. Further details of the experimental set-up are given elsewhere.[24] The samples with concentrations corresponding to an optical density of 1.4 at the excitation wavelength were prepared directly prior to the experiments. RR measurements were carried out by using a rotating cuvette to avoid photodecomposition. Under these conditions the samples were stable for ca. 30 min (Fe−O−O−H) and 10 min (Fe−O−O). The integrity of samples during the RR experiments was checked by comparing the consecutively measured RR spectra obtained with an integration time of 1 s. For improvement of the signal-to-noise ratio, the individual spectra were finally combined. The sum spectra obtained in this way represent measurements of a total accumulation time of between 10 and 40 s. After removal of the structureless background by polynomial subtraction, the spectra were analyzed by a band-fitting procedure using Lorentzian lineshapes.[25]

Synthesis of the Ligands: The trispicen, trispicMeen, and TPEN ligands were prepared according to previously described procedures.[8,11,20]

Syntheses of the Complexes: The complexes $[(TPEN)Fe](PF_6)_2$, $[(TPEN)Fe](ClO_4)_2$, $[(trispicMeen)FeCl]PF_6$ and [(trispicMeen)-FeCl]Cl were prepared as previously described.[8,17,20]

Synthesis of the Complex $[(TPEN)Fe]Cl_2 \cdot 0.5H_2O$: A solution of $FeCl_2 \cdot 4H_2O$ (0.49 mmol) in dry THF under argon was added to a solution of TPEN (0.51 mmol) in dry THF. The immediate yellow precipitate was collected by filtration (yield = 80%). − ESI MS: m/z = 240.2 $[\{(TPEN)Fe\}^{2+}]$, 515.1 $[\{(TPEN)FeCl\}^{+}]$ − UV/Vis (MeOH, 300 K): λ_{max} = 417 nm (ε = 10500 $м^{-1}.cm^{-1}$) − $C_{26}H_{28}Cl_2FeN_6 \cdot 0.5H_2O$ (560.31): calcd. C 55.73, H 5.22, N 15.0; found C 55.76, H 5.16, N 14.39.

Synthesis of the Complex $[(trispicen)FeCl]PF_6$: A solution of $FeCl_2 \cdot 4H_2O$ (0.30 mmol) in ethanol was added to a solution of trispicen (0.31 mmol) in ethanol. A yellow powder was obtained after addition of NH_4PF_6 (0.31 mmol) and collected by filtration (yield = 56%). − UV/Vis (MeOH, 300 K): λ_{max} = 395 nm (ε = 1900 $м^{-1}.cm^{-1}$).

[1] M. Sono, M. P. Roach, E. D. Coulter, J. H. Dawson, *Chem. Rev.* **1996**, *96*, 2841−2887.
[2] D. E. Benson, K. S. Suslick, S. G. Sligar, *Biochemistry* **1997**, *36*, 5104−5107.
[3] J. Stubbe, J. W. Kozarich, W. Du, D. E. Vanderwall, *Acc. Chem. Res.* **1996**, *29*, 322−330.
[4] J. W. Sam, X. J. Tang, J. Peisach, *J. Am. Chem. Soc.* **1994**, *116*, 5250−5256.
[5] C. Nguyen, R. J. Guajardo, P. K. Mascharak, *Inorg. Chem.* **1996**, *35*, 6273−6281.
[6] I. Lippai, R. S. Magliozzo, J. Peisach, *J. Am. Chem. Soc.* **1999**, *121*, 780−784.
[7] M. Lubben, A. Meetsma, E. C. Wilkinson, B. Feringa, L. Que, Jr, *Angew. Chem. Int. Ed. Engl.* **1995**, *34*, 1512−1514.
[8] I. Bernal, I. M. Jensen, K. B. Jensen, C. J. McKenzie, H. Toftlund, J. P. Tuchagues, *J. Chem. Soc., Dalton Trans.* **1995**, 3667−3675.

[9] C. Kim, K. Chen, J. Kim, L. Que, Jr, *J. Am. Chem. Soc.* **1997,** *119*, 5964−5965.
[10] M. E. de Vries, R. M. La Crois, G. Roelfes, H. Kooijman, A. L. Spek, R. Hage, B. L. Feringa, *Chem. Commun.* **1997**, 1549−1550.
[11] P. Mialane, A. Novorojkine, G. Pratviel, L. Azéma, M. Slany, F. Godde, A. J. Simaan, F. Banse, T. Kargar-Grisel, G. Bouchoux, J. Sainton, O. Horner, J. Guilhem, L. Tchertanova, B. Meunier, J. J. Girerd, *Inorg. Chem.* **1999**, *38*, 1085−1092.
[12] R. Y. N. Ho, G. Roelfes, B. L. Feringa, L. Que, Jr, *J. Am. Chem. Soc.* **1999**, *121*, 264−265.
[13] G. Roelfes, M. Lubben, K. Chen, R. Y. N. Ho, A. Meetsma, S. Genseberger, R. M. Hermant, R. Hage, S. K. Mandal, V. G. Young, Jr, Y. Zang, H. Kooijman, A. L. Spek, L. Que, Jr, B. L. Feringa, *Inorg. Chem.* **1999**, *38*, 1929−1936.
[14] K. B. Jensen, C. J. McKenzie, L. P. Nielsen, J. Z. Pedersen, H. M. Svendsen, *Chem. Commun.* **1999**, 1313−1314.
[15] S. Ahmad, J. D. McCallum, A. K. Shiemke, E. H. Appelman, T. M. Loehr, J. Sanders-Loehr, *Inorg. Chem.* **1988**, *27*, 2230−2233.
[16] F. Neese, E. I. Solomon, *J. Am. Chem. Soc.* **1998**, *120*, 12829−12848.
[17] A. J. Simaan, F. Banse, P. Mialane, A. Boussac, S. Un, T. Kargar-Grisel, G. Bouchoux, J. J. Girerd, *Eur. J. Inorg. Chem.* **1999**, 993−996.
[18] R. Y. N. Ho, G. Roelfes, R. Hermant, R. Hage, B. L. Feringa, L. Que, Jr, *Chem. Commun.* **1999**, 2161−2162.
[19] The magnetic susceptibility of a solid sample of [(TPEN)Fe]Cl_2 $0.5H_2O$ has been measured as a function of temperature . It clearly shows an $S = 2$ state from 300 K down to 10 K.
[20] H. R. Chang, J. K. McCusker, H. Toftlund, S. R. Wilson, A. X. Trautwein, H. Winkler, D. N. Hendrickson, *J. Am. Chem. Soc*. **1990**, *112*, 6814−6827.
[21] J. S. Griffith, *The Theory of Transition Metal Ions,* Cambridge University Press, London, **1961.**
[22] C. P. S. Taylor, *Biochim. Biophys. Acta* **1977**, *491*, 137−149.
[23] A. Veselov, H. Sun, A. Sienkiewicz, H Taylor, R. M. Burger, C. P. Scholes, *J. Am. Chem. Soc.* **1995**, *117*, 7508.
[24] H. Wackerbarth, U. Klar, W. Günther, P. Hildebrandt, *Applied Spectroscopy* **1999**, *53*, 283−291.
[25] S. Döpner, P. Hildebrandt, A. G. Mauk, H. Lenk, W. Stempfle, *Spectrochim. Acta* **1996**, *A51*, 573−584.

Received July 26, 1999
[I99276]